NANO-MICRO LETTERS

Vol. 1, No. 1
9-13 (2009)

Semiconducting single-walled carbon nanotubes synthesized by S-doping

Z. J. Li, L. Wang, Y. J. Su, P. Liu and Y. F. Zhang*

An approach was presented for synthesis of semiconducting single-walled carbon nanotubes (SWNTs) by sulfur (S) doping with the method of graphite arc discharge. Raman spectroscopy, UV-vis-NIR absorption spectroscopy and electronic properties measurements indicated the semconducting properties of the SWNTs samples. Simulant calculation indicated that S doping could induce convertion of metallic SWNTs into semiconducting ones. This strategy may pave a way for the direct synthesis of pure semiconducting SWNTs.

Keywords: S-doping; Single-wall; Carbon nanotubes; Semiconducting; Arc discharge

Citation: Z. J. Li, L. Wang, Y. J. Su, P. Liu and Y. F. Zhang, "Semiconducting single-walled carbon nanotubes synthesized by S-doping", Nano-Micro Lett. 1, 9-13 (2009). doi: 10.5101/nml.v1i1.p9-13

Over the past decades, single-walled carbon nanotubes (SWNTs) used as building blocks of nanoscale electronic devices have attracted great attention due to their quasi one-dimensional structure and unique properties [1-3]. Depending on their diameter and chirality, SWNTs can exhibit either metallic or semiconducting behavior. However, the chirality of nanotubes can not be controlled normally until now [4]. How to obtain purely semiconducting SWNTs (semi-SWNTs) becomes one of the major obstacles to the widespread applications of SWNTs for high performance electronics [5]. Several separation approaches for the enrichment of one certain electronic type of SWNTs have been developed, such as electrical breakdown [6-9], ultracentrifugation [10], selective plasma etching [5], electrophoresis [12] and selective chemical functionalization [6]. But the problem is that the post-treatments processes are tedious beyond controlled and often have the disadvantage of damaging or contaminating SWNTs samples [7,8]. Recently, preferential growth of Semi-SWNTs by chemical vapor deposition (CVD) methods by boron/nitrogen co-doping was reported to produce high percentage of Semi-SWNTs or a specific chirality distribution SWNTs [10-13]. These pioneering studies indicate the possibility for selective synthesis of Semi-SWNTs by heterodoping methode.

S contained compound has often been used as an additive in the synthesis of CNTs [14] for increasing the yield of SWNTs or DWNTs. Even, Denis et al [15] reported S doping could modify the electronic structure of the SWNTs by using first-principles calculations. Recently, we tested a technique for the synthesis of SWNTs by graphite arc discharge in hydrogen with S doping. The as-synthesized S-doped SWNTs showed purely semiconducting. Theory calculations elucidate that the metallic chirality SWNTs can be converted into semiconductors by proper S concentrations doping into the tube wall structure.

S-doped SWNTs were synthesized by arc discharge between two graphite electrodes in hydrogen atmosphere. The graphite electrodes were graphite rods of ~6 mm in diameter and made with high purity graphite, iron (5 at%) and S (0.1-2.0 at%). Briefly, the synthesis apparatus consists of graphite electrodes, a water-cooled trap, and a DC power supply which is capable of providing the voltage of 150 V and the current of 100 A. During DC arc discharge process, the distance between the graphite electrodes was maintained about 2 mm. The optimum

National Key Laboratory of Nano/Micro Fabrication Technology, Key Laboratory for Thin Film and Microfabrication of the Ministry of Education, Research Institute of Micro/Nanometer Science & Technology, Shanghai Jiaotong University, Shanghai 200240, PR China

*Corresponding author. Email: yfzhang@sjtu.edu.cn. Tel: +86 34205665, Fax: +86-021-34205665

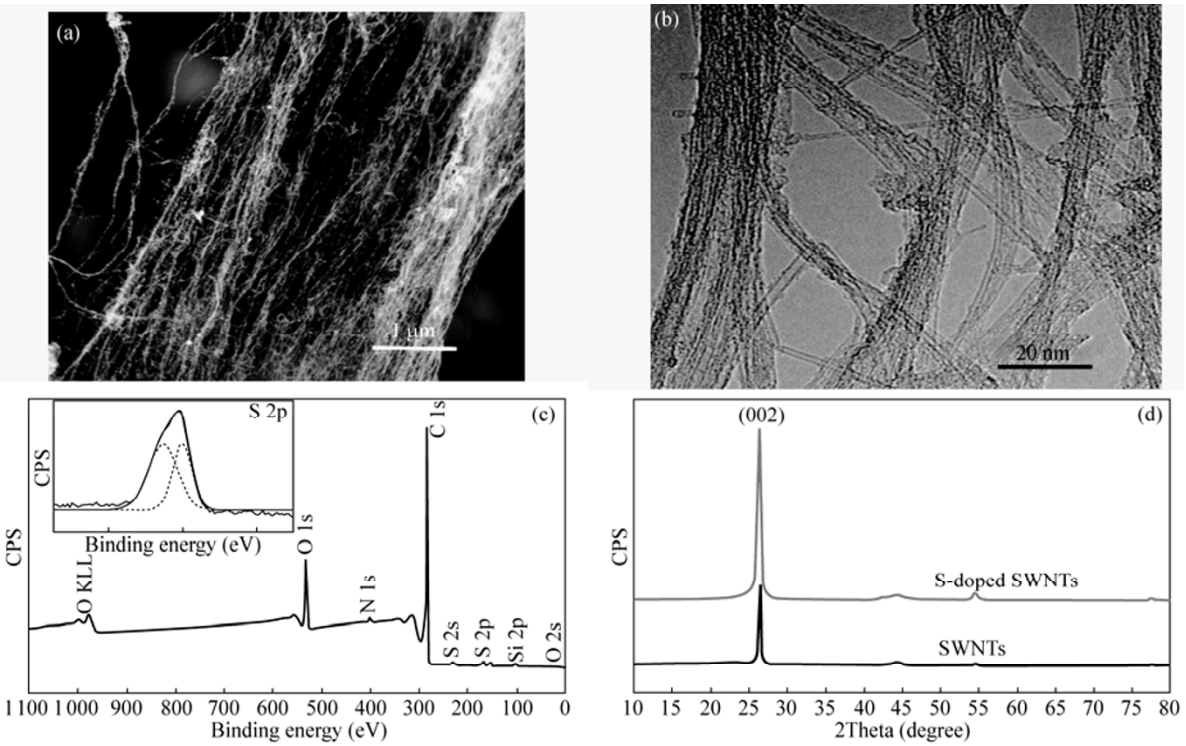

FIG. 1. (a) A typical SEM image of as-synthesized S-doped SWNTs. (b) HRTEM image of as-synthesized S-doped SWNTs. (c) XPS spectrum of the as-synthesized S-doped SWNTs. (d) XRD patterns of S-doped and undoped SWNTs.

parameters of current and voltage for the DC arc discharge were 40 A and 55 V respectively. A magnetic field of ~160 mT was applied to confine the discharge plasma, and aligned SWNTs thin film can be obtained by adjusting the orientation of the magnetic field.

The as-synthesized SWNTs have been characterized by scanning electron microscopy (SEM, JSM-7401F), high-resolution transmission electron microscopy (HRTEM; JEM2010), UV-vis-NIR absorption spectroscopy and Raman spectroscopy (by 514.5 and 632.8 nm excitation). X-ray photoelectron (XPS) was used to estimate the contents of sulfur and characterize their bonding environments. The electronic properties of the as-synthesized SWNTs have also been measured by fabricating CNT-FETs devices. The electrical properties were studied by two field effect configuration. One is thin film SWNTs FETs. The other is FETs based on several SWNTs bridging the two electrodes. The electrical properties of CNT-FETs were measured by Agilent 4156C.

Figure 1a shows the typical SEM image of as-synthesized SWNTs sample. It can be seen that the SWNTs with clean and smooth surface are homogenously distributed and entangled. HRTEM (Fig. 1b) provides direct evidence that the nanotubes were single-walled with the average diameter of ~1.2 nm. Figure 1c shows the XPS of as-synthesized SWNTs. Inset shows the high resolution S 2p XPS spectra, which has been curve-fitted by Voigt lines to detect bonding structure. In order to find whether S incorporated into the nanotubes, the surface layer of sample was etched away by Ar^+ sputtering for 3 min. The broad band can be deconvoluted into two bands at 169.2 and 167.6 eV, which can be assigned to the C-O and C-S bonding structures, respectively. The S concentration in SWNTs powders estimated to be 1.4 at %. Figure 1d is the XRD patterns of the S-doped SWNTs and undoped SWNTs. The major peak at 2θ=25.952º is corresponding to (002) reflections of polyaromatic. It is worth while noting that the intensity and half width of the diffraction at 25.952º increase after S doping.

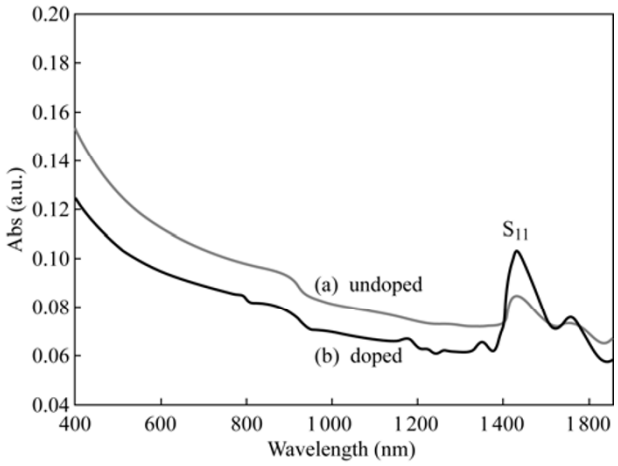

FIG. 2. UV-vis-NIR absorption spectroscopy of the undoped and doped samples.

These indicate that S doping induces partial aberration of the geometry structure of SWNTs while the crystal structure of SWNTs is unchanged after S doping.

Figure 2 and Fig. 3 show the typical optical spectra of an undoped SWNTs sample. The UV-vis-NIR absorption spectroscopy in Fig. 2 shows that several peaks in the semiconducting band arise from the electronic transitions between the first pair of van Hove singularities (vHs) in semiconducting SWNTs (S_{11} band) and the second pair (S_{22} band). The intensities of the S_{11} band transition peaks of the as-synthesized S-doped SWNTs sample are greatly dominant relative to the undoped SWNTs sample while the M_{11} band shows little change, which is indicative of a higher Semi-SWNTs content in the as-synthesized sample. Moreover, red shift of S_{11} band (main peak shift) indicates that the band gaps of the S-doped SWNTs changed probably. The radial breathing mode (RBM) region of SWNTs Raman spectra can be used to assign and quantitatively evaluate metallic and semiconducting nanotubes [16-18]. As-synthesized SWNTs samples were sonicated in ethanol for 10 min, and then the suspensions were dropped on glass slides and dried in air. Figure 3 shows the meseaured Raman spectra in RBM region. The intensities of semiconducting S33 (514 nm excitation) and S22 (633 nm excitation) from as-synthesized S-doped SWNTs increase, whereas the intensities of the peak attributed to metallic SWNTs were disappear.

For better understanding the S-doping effects into metallic SWNT structure, calculations are carried out with the density functional theory implemented provided by Dmol^3 package [19]. Figure 4 shows the band structures by first-principles calculations for an S-doped (7, 7) metallic SWNT. The all-electron Kohn-Sham wave functions were expanded in the local atomic orbital (double numerical polarization, DNP) basis set and generalized gradient approximation (GGA) of Perdew-Burke-Ernzerhof (PBE) for the exchange-correlation potential [20]. The Monkhorst-Pack scheme was used in the Brillouin zone with 1×1×10 for all the geometry optimization and total energies calculations [21]. Self-consistent field procedure was done with a convergence criterion of 10^{-5} a.u. on the energy and electronic properties. As shown in Fig. 4a, a typical metallic (7, 7) SWNT has no energy band at the Fermi level. The band structures of S-doped SWNTs in different concentrations show that the energy gaps of about 0.24 eV for 0.71% (Fig. 4b) and about 0.29 eV for 1.43% (Fig. 4c) open at Fermi level. It is suggested that metallic SWNTs can be converted into semiconductors by sulfur doping with proper S concentrations.

SWNTs field effect transistors (FET) were used to test the electronic properties of the S-doped SWNTs. SWNTs solutions

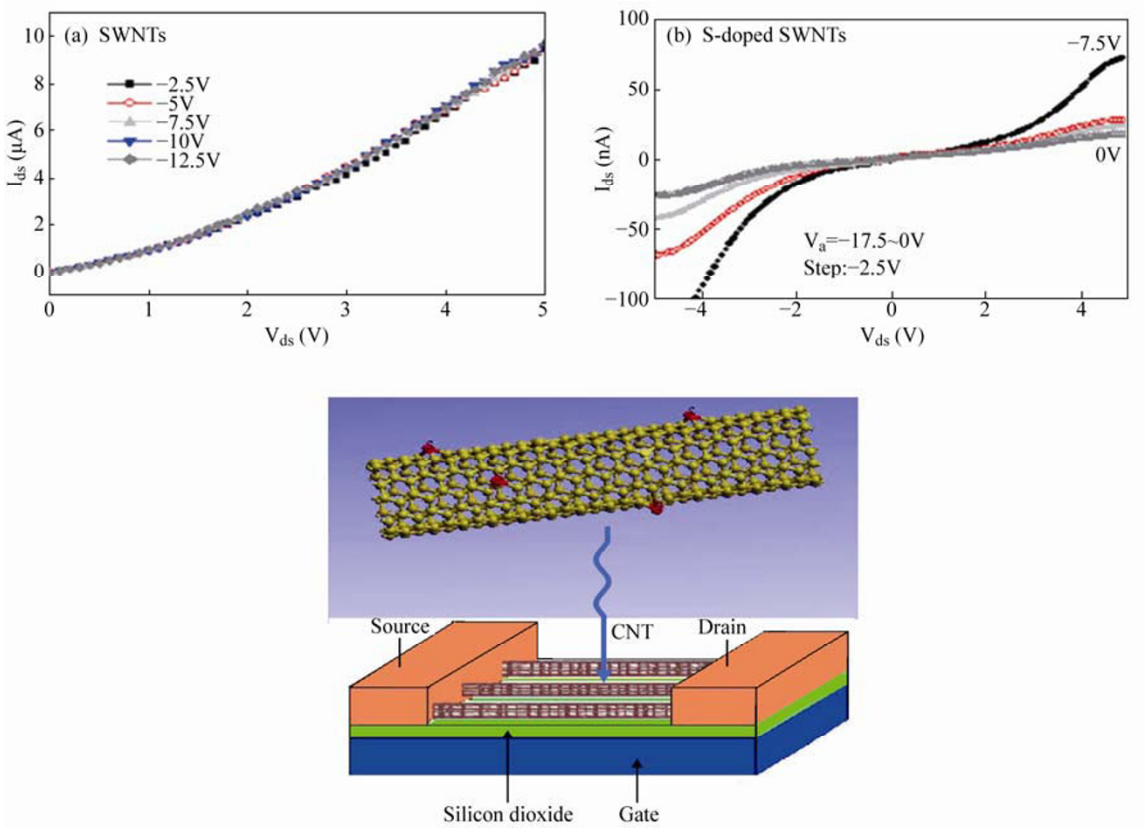

FIG. 5. (a) Output characteristic of as-synthesized SWNTs FET. (b) Transfer curve of the drain current vs gate voltage measured at a drain voltage of 0.4 V, (c) the schematic of structure of thin film transistor.

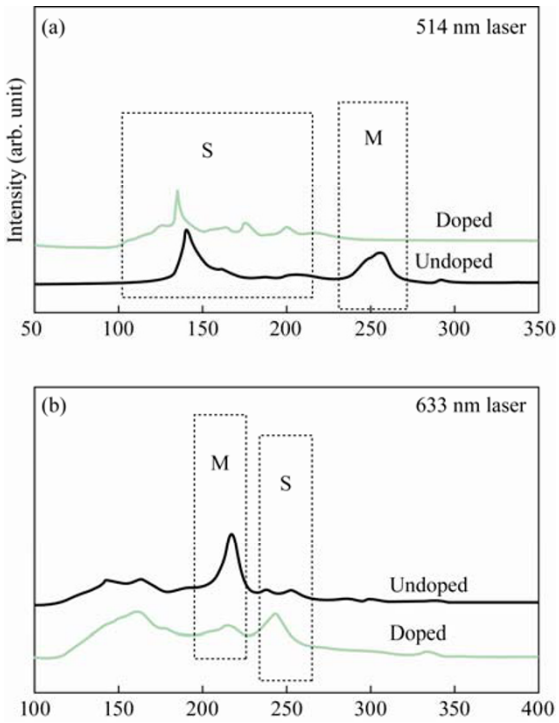

FIG. 3. RBM of Raman spectra of the undoped and doped samples using laser beams of excitation wavelengths: (a) 514 nm, and (b) 633 nm.

were spin coated on a Si/SiO_2 wafer to form a random SWNTs thin film. The SiO_2 surface layer of 80 nm thick acted as a back gate electrode. On top of the films, source (S) and drain (D) electrodes with a channel distance ~10 μm were made of 10 nm Ti, followed by 30 nm Au by electron beam lithography technique. The schematic of the SWNTs field effect transistors (FET) structure and their electronic properties curves are shown in Fig. 5. Figure 5a demonstrates the source-drain current increase with increasing negative gate voltage. Figure 5b is the transfer characteristic of as-synthesized S- doped SWNTs-FET which shows that the on/off ratio is more than 10^3 by sweeping gate voltage at room temperature. In contrast, similar thin film field-effect configuration based on the undoped SWNTs sample shows the on/off ratio of less than 10, which means that the undoped sample may contain a lot of M-SWNTs.

CNT-FETs device based on the as-synthesized randomly networked S-doped SWNTs film not just a few CNTs showed a typical field effect characteristic feature, in which the drain current increased with increasing negative gate voltage, this reveals that the S-doped SWNTs is a p-type semiconductor [22-34]. A schematic of the transistor is shown as an inset in Fig. 5c. This result is consistent with that of the first-principles calculations, in which the formation energies of same-diameter Semi-SWNTs are lower than those of M-SWNTs because of the electronic energy gain resulting from the band gap opening and

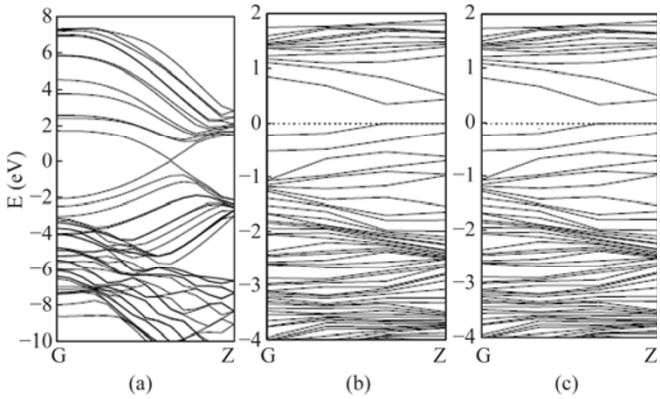

FIG. 4. Band structures of S-doped SWCNTs at different sulfur atom concentrations: (a) pristine, (b) 0.71% and (c) 1.43 %, respectively.

the higher chemical reactively of M-SWNTs due to more abundant delocalized electronic states [23, 24].

In summary, a new method was identified for synthesizing semiconducting SWNTs by graphite arc discharge and S-doping in hydrogen atmosphere. Experimental data and theoretical calculations indicate that the electric properties of S-doped SWNTs are typical semiconductors. Typical FET device performance was shown from S-doped SWNTs FETs. S-doping method has opened a new route for mass production of semiconducting SWNTs.

The authors thank for the supports of theoretical calculations from Prof. X. S. Chen and Prof. W. Lu at National Laboratory for Infrared Physics, CAS. This work is supported by National Natural Science Foundation of China No. 50730008, Shanghai Science and Technology Grant No. 0752nm015 and National Basic Research Program of China No. 2006CB300406.

Received 20 August 2009; accepted 5 September 2009; published online 15 October 2009.

References

1. R. H. Baughman, A. A. Zakhidov and W. A. de Heer, Science 297, 787 (2002). doi:10.1126/science.1060928
2. L. M. Dai and A. W. H. Mau, Adv. Mater. 13, 899 (2001). doi:10.1002/1521-4095(200107)13:12/13<899::AID-ADMA899>3.0.CO;2-G
3. P. Avours, Z, Chen and V. Perebeinos, Nature Nanotech. 2, 605 (2007).
4. E. S. Snow, P. M. Campbell and M. G. Ancona, Appl. Phys. Lett. 86, 033105 (2005). doi:10.1063/1.1854721
5. J. Lu, L. Lai, G. Luo, J. Zhou, R. Qiu and D. Wang, Small 3, 1566 (2007). doi:10.1002/smll.200700127
6. P. C. Collins, M. S. Arnold and P. Avouris, Science 292,

706 (2001). doi:10.1126/science.1058782

7. R. Seidel, A. P. Graham, E. Unger, G. S. Duesberg, M. Steinhoegl, F. Kreupl and W. Hoenlein, Nano Lett. 4, 831 (2004). doi:10.1021/nl049776e
8. Y. X. Zhou, A. Gaur, S. H. Hur C. Kocabas, M. A. Meitl, M. Shim and J. A. Rogers, Nano Lett. 4, 2031 (2004). doi:10.1021/nl048905o
9. C. X. Chen, Z.Y Hou, X. Liu, E. S. W. Kong, J. P. Miao and Y. F. Zhang, Phys. Lett. A 366, 474 (2007). doi:10.1016/j.physleta.2007.02.089
10. A. Javey, J. Guo, Q. Wang, M. Lundstrom and H. J. Dai, Nature 424, 654 (2003). doi:10.1038/nature01797
11. G. Y. Zhang, P. F. Qi, X. R. Wang, Y. Lu, X. Li, R. Tu, S. Bangsaruntip, D. Mabb, L. Zhang and H. J. Dai, Science 314, 974 (2006). doi:10.1126/science.1133781
12. R. Krupke, F. Hennrich, H. von Lohneysen and M. M. Kappes, Science 301, 344 (2003). doi:10.1126/science.1086534
13. D. Chattopadhyay, L. Galeska and F. Papadimitrakopoulos, J. Am. Chem. Soc. 125, 3370 (2003). doi:10.1021/ja028599l
14. C. P. Buckley and D. C. Jones, Polymer 36, 3301 (1995). doi:10.1016/0032-3861(95)99429-X
15. P. A. Denis, R. Faccio and A. W. Mombru, Chem. Phys. Chem. 10, 715 (2009). doi:10.1002/cphc.200800592
16. Y. M. Li, D. Mann, M. Rolandi, W. Kim, A. Ural and S. Hung, Nano Lett. 4, 317 (2004). doi:10.1021/nl035097c
17. L. T. Qu, F. Du and L. M. Dai, Nano Lett. 8, 2682 (2008). doi:10.1021/nl800967n
18. X. L. Li, X. M. Tu, S. Zaric, K. Welsher, W. S. Seo, W. Zhao and H. J. Dai, J. Am. Chem. Soc. 129, 15770 (2007). doi:10.1021/ja077886s
19. B. Deller, J. Chem. Phys. 113, 7756 (2000). doi:10.1063/1.1316015
20. J. P. Perdew, K. Berke and M. Ernzerhof, Phys. Rev. Lett. 77, 3865 (1996). doi:10.1103/PhysRevLett.77.3865
21. H. J. Monkhorst and J. D. Pack, Phys. Rev. B 13, 5188 (1976). doi:10.1103/PhysRevB.13.5188
22. Z. Xu, W. G. Lu, W. L. Wang, C. Z. Gu, K. Liu, X. D. Bai, E. Wang and H. J. Dai, Adv. Mater. 20, 3615 (2008). doi:10.1002/adma.200800830
23. J. Zhang and C. Pan, J. Phys. Chem. C. 112, 13470 (2008). doi:10.1021/jp8034852.
24. M. Keidar, I. Levchenko, T. Arbel, M. Alexander, A. M. Waas and K. K. Ostrikov, J. Appl. Phys. 103, 094318 (2008). doi:10.1063/1.2919712
25. W. J. Kim, M. L. Usrey and M. S. Strano, Chem. Mater. 19, 1571 (2007). doi:10.1021/cm061862n
26. H. Kataura, Y. Kumazawa, Y. Maniwa, I. Umezu, S. Six and Y. Achiba, Synth. Met. 103, 2555 (1999). doi:10.1016/S0379-6779(98)00278-1
27. C. X. Chen, L. Y. Liu, Y. Lu, E. S. W. Kong and Y. F. Zhang, Carbon 45, 436 (2007). doi:10.1016/j.carbon.2006.08.021
28. W. J. Kim, M. L. Usrey and M. S. Strano, Chem. Mater. 19, 1571 (2007). doi:10.1021/cm061862n
29. H. L. Zhang, Y. Q. Liu, L. C. Cao, D. C. Wei, Y. Wang, H. Kajiura, Y. M. Li, K. Noda, G. F. Luo, L. Wang, J. Zhou, J. lu and Z. X. Gao, Adv. Mater. 21, 813 (2009). doi:10.1002/adma.200800703
30. C. X. Chen, L. J. Yan, E. S. W. Kong and Y. F. Zhang, Nanotechnology 17, 2192 (2006). doi:10.1088/0957-4484/ 17/9/019
31. C. X. Chen, D. Xu, E. S. W. Kong and Y. F. Zhang, IEEE Electron Device Lett. 27, 852 (2006). doi:10.1109/LED.2006.882530
32. C. X. Chen, Y. Lu, E. S. W. Kong, Y. F. Zhang and S. T. Lee, Small 4, 1313 (2008). doi:10.1002/smll.200701309
33. H. Park, J. Zhao and J. P. Lu, Nanotech. 16, 635 (2005). doi:10.1088/0957-4484/16/6/003
34. Y. Li, S. Peng, D. Mann, J. Cao, R. Tu, K. J. Cho and H. J. Dai, J. Phys. Chem. B. 109, 6968 (2005). doi:10.1021/jp050868h